

Quantum complexity and localization in random and time-periodic unitary circuits

Himanshu Sahu^{1,2,3,†}, Aranya Bhattacharya^{4,§} and Pingal Pratyush Nath^{5,‡}

¹*Perimeter Institute for Theoretical Physics, Waterloo, ON, N2L 2Y5, Canada.*

²*Department of Physics and Astronomy and Institute for Quantum Computing, University of Waterloo, ON N2L 3G1, Canada.*

³*Department of Physics and Department of Instrumentation & Applied Physics,
Indian Institute of Sciences, C.V. Raman Avenue, Bangalore 560012, India.*

⁴*Institute of Physics, Jagiellonian University, Lojasiewicza 11, 30-348 Kraków, Poland.*

⁵*Centre for High Energy Physics, Indian Institute of Science, C.V. Raman Avenue, Bangalore 560012, India.*

We study the growth and saturation of Krylov spread (K-) complexity under random quantum circuits. In Haar-random unitary evolution, we show that, for large system sizes, K-complexity grows linearly before saturating at a late-time value of $D/2$, where D is the Hilbert space dimension, at timescales $\sim D$. Our numerical analysis encompasses two classes of random circuits: brick-wall random unitary circuits and Floquet random circuits. In brick-wall case, K-complexity exhibits dynamics consistent with Haar-random unitary evolution, while the inclusion of measurements significantly slows its growth down. For Floquet random circuits, we show that localized phases lead to reduced late-time saturation values of K-complexity, forbye we utilize these saturation values to probe the transition between thermal and many-body localized phases.

Introduction. — Understanding the complexity of quantum states and operators is relevant to a wide range of settings, from quantum many-body physics through quantum gravity to quantum computation [1–14]. In many-body physics, insights into the buildup of complexity in the time evolution of an initial local observable, known as operator growth, have inspired new ways of probing the dynamics of thermalization [15, 16]. Out-of-time-order correlators (OTOCs) [2, 17, 18], a quantitative tool for measuring operator growth, obeys a dynamical bound arising from unitarity and analyticity [9]. It is shown that in a version of quantum gravity known as anti-de-Sitter space/conformal field theory (AdS/CFT) duality, the black holes saturate this bound [7]. Similar to black holes, OTOCs saturates the bound in models such as the so-called Sachdev-Ye-Kitaev (SYK) model which has given rise to holographic dual description with black holes [19–21].

In quantum computing, the complexity of pure states is defined as the size of the smallest circuit that produces the state from a product state, while the complexity of a unitary is defined as the smallest circuit that approximates the unitary. This notion of quantum circuit complexity has recently gained interest due to connections between gate complexity and holography in AdS/CFT correspondence [22–26]. It is conjectured that in the bulk theory, the wormhole’s volume is dual to the boundary state’s quantum complexity, whose growth has been proved for the random unitary circuits [27].

Recently, the notion of state and operator complexity based on Krylov basis (which is referred to as ‘quantum complexity’ for convenience) defined using the generator of evolution operator has been extensively studied as a probe of information scrambling [28–39]. Operator complexity (known as Krylov complexity) is conjectured to grow at most exponentially in nonintegrable systems and can be used to extract the Lyapunov exponent, there-

fore, establishing a connection with OTOCs [28, 40]. On the other hand state complexity (known as spread complexity), a generalization of Krylov complexity for quantum states, is used as a probe to study quantum chaos and topological phase transitions [30, 36, 41]. Furthermore, since by construction this notion of complexity measures the delocalization of a wave function in the Krylov basis with time, it also captures the localization of the wavefunction by suppression in the complexity saturation value [37].

Despite a number of investigations in varying quantum systems, how the Krylov spread complexity in systems with discrete-time evolution behaves remains an open question [42]. In this Letter, we study quantum complexity in various classes of random quantum circuits. Quantum circuits built from local unitary gates (and randomized local measurements) are a new playground for quantum many-body physics and a tractable setting to explore universal collective phenomena far from equilibrium. These models have shed light on longstanding questions about thermalization and chaos, and on the underlying universal dynamics of quantum information and entanglement [43–56].

In random unitary circuits (RUCs) that consists of local Haar-random unitaries, any quantum state evolves towards increasingly entangled states characterized by an extensive scaling of entanglement entropy with system volume. In presence of measurements which occur repeatedly during the evolution at a fixed rate, the system undergoes a phase transition from volume-to-area-law of entanglement entropy scaling for infrequent and frequent measurement rates, respectively [46, 51]. Another class of random quantum circuits capturing important physical insights are the time-periodic ones, namely *Floquet quantum circuits*, where each time-step is repeated with the same random instances. In previous studies, classes of Floquet unitary circuit have been

shown to exhibit localized phase such as Anderson localization (AL) and many-body localization (MBL) [57].

In this paper, we study the quantum complexity in these two aforementioned classes of quantum circuits — completely random unitary circuits with and without randomized measurements, and Floquet random unitary circuits (where the random realization of the first timestep is repeated in all further timesteps). In random unitary circuits, the complexity undergoes a transition from linear growth at early time to sublinear and saturates at exponentially late times in system-size. We find that the complexity growth slows down and the saturation-time increases ‘significantly’ under randomized local measurements above a threshold rate of measurement.¹ In Floquet unitary circuits, we find the suppression of late-time complexity-saturation value in localized phases. Therefore, our notion of complexity can be used as probe for phase transition from thermal to MBL and Anderson localization phases. To this end, our work therefore provides the first ever explicit circuit realization of the Krylov spread complexity, which probes system size, randomized measurement rate, and the onset of localizing phases.

Model.— We consider discrete time evolution of two classes of one-dimensional quantum circuit models with N qubits — Random unitary circuits (RUCs) and Floquet unitary circuits (FUCs). For each time step, there is a unitary evolution operator $U_t = U(t; t-1)$, under which a pure state evolves as $|\psi(t)\rangle = U_t|\psi(t-1)\rangle$. The unitary evolution U_t is taken to be local unitary gates which are arranged in a bricklayer pattern:

$$U_t = \left(\prod_{x \in \text{odd}} \mathcal{U}_{(x,x+1),2t+1} \right) \left(\prod_{x \in \text{even}} \mathcal{U}_{(x,x+1),2t} \right) \quad (1)$$

$$= \mathcal{U}_t^{(o)} \cdot \mathcal{U}_t^{(e)}$$

where $\mathcal{U}_{(x,x+1),\tau}$ is the gate on link $(x, x+1)$ at time step τ . In random unitary circuits, the local unitary gates $\mathcal{U}_{x,t}$ are *Haar-random* unitary gates. We note that even the minimal brickwork circuit above possesses one basic structure, which is the spatial locality of the interaction, which is natural in quantum information and as toy models for black holes [5, 6, 8, 58]. The quantum circuit complexity of such system is shown to grow linearly, before saturating when the number of applied gates reaches threshold that grows exponentially with the number of qubits [27]. Furthermore, the scrambling dynamics exhibits similarities to the large- N or semiclassical case, but wavefront broadens diffusively [17]. We

further introduce *nonunitary* dynamics by puncturing the unitary circuit with local randomized single-qubit measurements. Measurements are done on a fraction p of all sites. Under the measurement, the wave function transforms as

$$|\psi\rangle \rightarrow \frac{M_\alpha |\psi\rangle}{\|M_\alpha |\psi\rangle\|} \quad (2)$$

where $\{M_\alpha\}$ are a set of linear *generalized measurement* operators satisfying $\sum_\alpha M_\alpha^\dagger M_\alpha = 1$. Under such a measurement, the process described by Eq. (2) is probabilistic, with outcome α happening with probability $p_\alpha = \langle \psi | M_\alpha^\dagger M_\alpha | \psi \rangle$. In our study, we will choose these *generalized measurement* operators to be mutually orthogonal projectors, that is $M_\alpha \rightarrow P_\alpha$, with $P_\pm = (1 \pm Z)/2$ measuring the Z component of the spin of individual qubits. Such projectors satisfy $P_\alpha P_\beta = \delta_{\alpha\beta} P_\alpha$ and $\sum_\alpha P_\alpha = 1$. This model undergoes a phase transition at a finite value of $p = p_C$ from volume- and area-law entanglement [43].

In Floquet unitary circuits, the evolution is made time-periodic $U_t = U_{t+1}$, i.e., the two layers are repeated identically in the spirit of Floquet evolution. We consider several variations of Floquet evolution with a unitary circuit, which was previously shown to exhibit localized phases [57]. The scenarios we consider are the following:

(A) *Gaussian circuits:* We consider N fermionic pairs (a_i, a_i^\dagger) satisfying $\{a_i, a_j^\dagger\} = \delta_{ij}$. We begin by defining a set of Hermitian fermionic operators given by

$$q_i = \frac{1}{\sqrt{2}}(a_i^\dagger + a_i) \quad \text{and} \quad p_i = \frac{i}{\sqrt{2}}(a_i^\dagger - a_i) \quad (3)$$

referred to as Majorana modes. Turning to the covariance matrix Ω , if we choose the Majorana basis $\xi^a \equiv (q_1, p_1, q_2, p_2 \dots q_N, p_N)$,

$$\Omega^{ab} = -i \text{Tr}(\rho[\xi^a, \xi^b]). \quad (4)$$

The covariance matrix provides a straightforward framework for discussing the corresponding group of unitary transformations for fermionic Gaussian states. In this context, we focus on Gaussian circuits that map Gaussian states to Gaussian states. The most general unitary operation acting on the covariance matrix is represented by an orthogonal transformation $O \in O(2N)$. We specifically consider a subclass of these unitary transformations, generated by quadratic Hamiltonians, which correspond to special orthogonal transformations $O \in \text{SO}(2N)$ [59, 60].

With this, the time evolution operator is given by an orthogonal transformation $O \in O(2N)$ built of random

¹ While our naive numerics suggest that this threshold is near $p = 0.5$ supporting previous results on complex-uncomplex transition in , a more precise numerical analysis shows that this value is not strictly 0.5, but system size dependent.

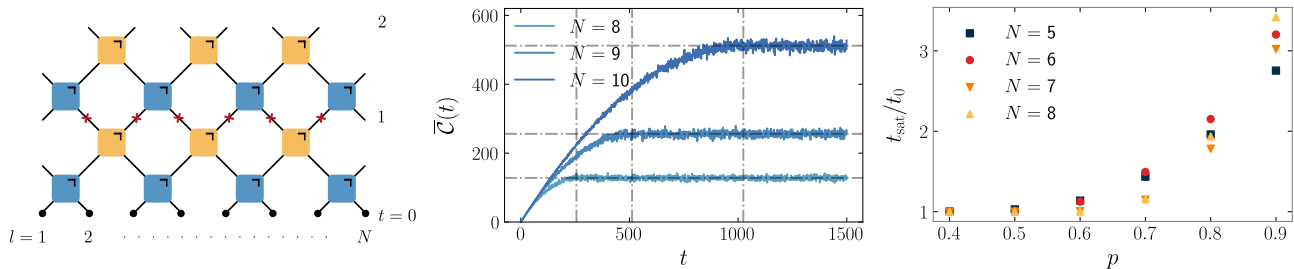


FIG. 1. **Left:** Illustration of random unitary circuit model consists of N qubits. The bricks represents local unitary operation arranged in brickwork manner. A single evolution steps consists of two-layers *i.e.* odd (blue) and even (yellow) of unitaries. The cross in red represents the local measurement on qubit. **Center** The disordered spread-complexity $\bar{C}(t)$ calculated for RUCs where the local unitaries are random Haar as a function of time steps t . There is early time transition from linear to sublinear complexity which eventually saturates at late time. The saturation time t_{sat} scales exponentially with system-size $t_{\text{sat}} \sim 2^N$ to a saturation value \bar{C}_{∞} also exponential in system-size $\sim 2^N/2$. **Right:** The ratio of saturation time at measurement rate p to the saturation time $p = 0$, plotted as a function of p computed for system-sizes $N = 5, 6, 7, 8$. The average is taken over 2000 copies.

two-site operations $P_i, Q_i \in O(4)$,

$$U_t = G \left(\bigoplus_{i=1}^{N/2} Q_i \right) G^T \left(\bigoplus_{i=1}^{N/2} P_i \right) \quad (5)$$

where

$$G = \begin{pmatrix} 0 & & \mathbb{1}_2 \\ \mathbb{1}_2 & 0 & \\ 0 & \ddots & \ddots \\ & & \mathbb{1}_2 & 0 \end{pmatrix} \quad (6)$$

takes care of circularly shifting $\bigoplus Q_i$ by one site, and ensures periodic boundary condition. Given the block diagonal form of the evolution operator, the two-site operations P_i are coupling between sites $2i-1$ and $2i$. The time average of covariance matrix can be used to assess long-time behavior of a typical state. It is shown that the inhomogeneous evolution exhibits Anderson localization; an initially localized impurity stays localized. On the other hand, the homogeneous evolution results in thermalization [57].

(B) *Spins:* The spin system that we consider is periodic version of random unitary circuit, where local unitary gates \mathcal{U} are drawn from different probability distributions with the common property of single-site Haar invariance. In other words, any transformation of a \mathcal{U} of the form

$$\mathcal{U} \leftrightarrow (w_1 \otimes w_2) \cdot \mathcal{U} \cdot (w_3 \otimes w_4) \quad (7)$$

does not affect averages $\langle \dots \rangle$, for arbitrary choice of single-qubit operator w_i .

Method.— Consider the evolution of initial state $|\psi(0)\rangle$ under discrete-time dependent unitary evolution such that $|\psi(t)\rangle = U_t |\psi(t-1)\rangle$, where $t = 1, 2, \dots$. We define the Krylov basis by choosing $|K_0\rangle = |\psi(0)\rangle$ and

then recursively orthogonalizing each $|\psi(t)\rangle$ with all the $|K_i\rangle$ for $i < t$ [29, 61]. At any t , we can expand the state $|\psi(t)\rangle$ in Krylov basis as

$$|\psi(t)\rangle = \sum_{n=0}^D \phi_n(t) |K_n\rangle, \quad (8)$$

where D is dimension of Hilbert space, and $\phi_n(t) = \langle K_n | \psi(t) \rangle$. We define the spread complexity of the state as the average position of the distribution on the ordered Krylov basis:

$$\mathcal{C}(t) = \sum_{n=0}^D n |\phi_n(t)|^2. \quad (9)$$

Analogously, we can define the Krylov complexity (K-complexity) of the operator, which evolves under discrete-time evolution $O_t = U_t^\dagger O_{t-1} U_t$. As before, the Krylov basis is obtained by choosing $|K_0\rangle = O_o$ and then recursively orthogonalizing each O_t with all the $|K_i\rangle$ for $i < t$. At any t , we can expand the operator O_t in Krylov basis as

$$O_t = \sum_{n=0}^{D^2} \varphi_n(t) |K_n\rangle \quad (10)$$

where $\varphi_n(t) = \langle K_n | O_t \rangle$. We define the K-complexity as

$$\mathcal{K}(t) = \sum_{n=0}^{D^2} n |\varphi_n(t)|^2. \quad (11)$$

RESULTS

Consider the state evolution under random haar unitary $\mathcal{U} \in \mathcal{C}^{D \times D}$. This results in set of random haar state

$\{|\psi_i\rangle\}_{i=0}^m$. We will assume that the Hilbert space dimension D is sufficiently larger than m . For a Haar-random quantum state $|\psi\rangle$ in a high-dimensional Hilbert space, the probability amplitudes $\langle x|\psi\rangle \equiv z_x$ (where $|x\rangle$ are basis states) follow the probability distribution

$$\Re(z_x) \sim \mathcal{N}\left(0, \frac{1}{2D}\right) \quad \Im(z_x) \sim \mathcal{N}\left(0, \frac{1}{2D}\right) \quad (12)$$

where $\mathcal{N}(0, \sigma^2)$ denotes a Gaussian distribution with mean 0 and variance σ^2 . The measure probability $p_x = |z_x|^2$ follows the Porter-Thomas distribution $P(p_x) = D e^{-D p_x}$. For two independent Haar-random vectors $|\psi\rangle$ and $|\phi\rangle$, it follows $\mathbb{E}[|\langle\psi|\phi\rangle|^2] = 1/D$ and $\text{Var}(|\langle\psi|\phi\rangle|^2) = 1/(D^2 + D) \sim 1/D^2$ for large D . Consider the set of orthonormal vectors $\{|\phi_i\rangle\}_{i=0}^m$ calculated using recursive orthogonalization. Then,

$$\mathbb{E}(|\langle\phi_i|\psi_n\rangle|^2) = \begin{cases} 1/D & i < n \\ 1 - (n-1)/D & i = n \end{cases} \quad (13)$$

where we used the normalization condition $\sum_i^n \mathbb{E}(|\langle\phi_i|\psi_n\rangle|^2) = 1$. It follows that

$$\mathbb{E}(\mathcal{C}(t)) = t - \frac{t(t-1)}{2D} \quad t < D \quad (14)$$

It follows that for $D \rightarrow \infty$, the complexity grows linearly with time. In finite system, the complexity saturates at exponentially late times $t_s = D-1$ to a value $\mathbb{E}(\mathcal{C}(t_s)) = D/2$, which is generic in many-body chaotic systems and quantum circuit complexity.

In Fig. 1(center), we show numerically computed complexity for the system-sizes $N = 8, 9, 10$ for local RUCs with brickwork structure. Unless otherwise mentioned, we will perform the average over the large number of sample copies so that quantities are well-converged. In numerical calculations, the initial state is a product state $|\psi(0)\rangle = |\uparrow\downarrow\uparrow\downarrow \dots\rangle$. However, taking any other states produces the same feature in the complexity profile, suggesting that it is independent of the initial state. We find that the complexity profile obeys result (Eq. (14)) derived for the RUCs.

In monitored RUCs, the Krylov basis constructed from orthogonalization of span of vectors

$$\mathfrak{R}_1 = \{|\psi(0)\rangle, M\mathcal{U}_1^{(o)}M\mathcal{U}_1^{(e)}|\psi(0)\rangle, \dots\} \quad (15)$$

where M represents measurement operation performed at probability rate p . In Fig. 1(right), we compute the saturation-time with increasing measurement rate p for system-sizes $N = 5, 6, 7, 8$. With increasing measurements, the system takes more and more time to acquire the complete orthonormal basis. A limiting case corresponding to $p = 1$ is studied in supplementary material for the haar-random circuit to bound the saturation time. It is easy to see from Fig. 1 (right) that upto

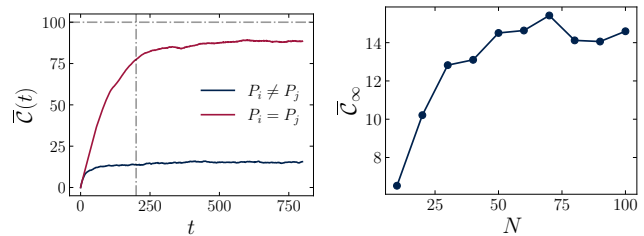


FIG. 2. **Left:** The disorder-averaged spread complexity $\bar{\mathcal{C}}(t)$ calculated for the initial product state and $N = 100$ fermionic pairs. The two-site operations P_i, Q_i corresponds to special orthogonal transformation $\text{SO}(4)$. The late-time saturation value is suppressed in inhomogeneous setting as result of Anderson localization. **Right:** The late-time saturation value plotted for varying system-size in inhomogeneous setting. As system-size increases the saturation value becomes constant.

certain value of $p = p_{\text{thr}}$, the saturation value remains invariant of the rate of measurement. This essentially means that the y -axis of the plot, namely t_{sat}/t_0 is 1 upto p_{thr} .² Our numerics suggest that this p_{thr} is close to but more precisely ≥ 0.5 in a system-size dependent way. The explanation for this is that after a certain rate of measurement, the system evolution is hindered by a higher rate of measurement. While this can be a version of quantum Zeno effect resulting in a slower state evolution, the effects becoming significant only after a certain measurement rate p_{thr} is suggestive of a qualitative similarity to that of [43, 62].

We now move to two classes of Floquet unitary circuits, namely Gaussian circuits and spins.

(A) *Gaussian circuits.*— In Fig. 2, we show the spread complexity associated with inhomogeneous and homogeneous settings. In homogeneous case where the time evolution O is 2-site-translation invariant, randomness is the same for all sites $P_i = P_j$ and $Q_i = Q_j$. We find that the spread of complexity exhibits a lower value of late-time saturation in the inhomogeneous case compared to the homogeneous case, which is reminiscent of Anderson localization. The suppression value $\bar{\mathcal{C}}_\infty$ takes up a constant in thermodynamics limit $N \rightarrow \infty$.

(B) *Spins.*— To begin with we consider the local unitary gates \mathcal{U} to be drawn from random Haar. In Fig. 3, we present numerical results for the spread complexity. The complexity profile remains similar to a random unitary case, except it features a peak before saturating.

The local unitary \mathcal{U} drawn from random Haar are highly entangling operators, therefore, move information that is initial localized in one site across the chain. On the other hand, MBL can typically requires strong

² Here t_0 is the saturation time 2^N for the N -qubit random unitary circuit without any measurements.

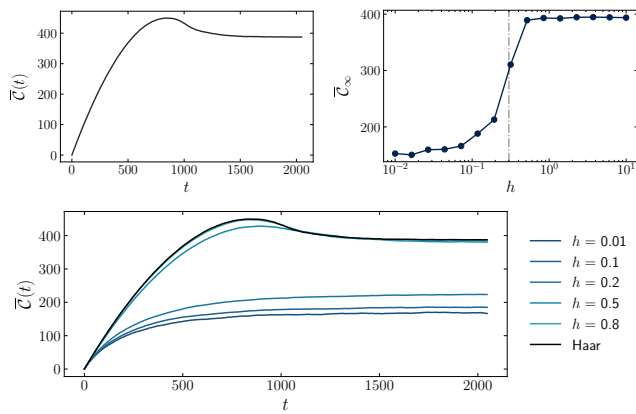


FIG. 3. The disordered spread complexity $\bar{\mathcal{C}}(t)$ for unitaries distributed according to Eq. (16) with random coupling strength h . For strong coupling, the late-time saturation is exponential in degrees of freedom showing the thermalization of system. In contrast, the late-time displays localization at weak coupling and the system displays localization.

random potential relative to the coupling [63]. To witness the MBL [57], we cast every unitary in $\mathcal{U}(4)$ as

$$(u_1 \otimes u_2) e^{ia\sigma_x \otimes \sigma_x + ib\sigma_y \otimes \sigma_y + ic\sigma_z \otimes \sigma_z} (u_3 \otimes u_4) \quad (16)$$

where $u_i \in \mathcal{U}(2)$ and coefficients $a, b, c \in \mathbb{R}$. The probability distribution for all two-qubit operators $\mathcal{U} \in \mathcal{U}(4)$ composing the time evolution operator is defined by Eq. 16, drawing each u_i from the Haar measure for $\mathcal{U}(2)$ and a, b, c uniformly from the interval $[-h, h]$.

In Fig. 3 we show numerics for $\bar{\mathcal{C}}(t)$ for distributions with various coupling strengths h . We find a crossover from thermalization for large coupling and localization for small coupling as evident from late-time saturation value $\bar{\mathcal{C}}_\infty$. The MBL transition can be extracted from $\bar{\mathcal{C}}_\infty$ as a function of h . In Fig. 3, the transition occurs at value $h_0 \approx 0.3$ independent of system-size which matches with previous studies [57].

Discussion.— In this paper, we study the state complexity in various classes of random unitary circuits. We show that the complexity undergoes a transition from linear to sublinear growth in random Haar unitaries, before saturating which scale exponentially with the number of qubits. Interestingly, the exponential scaling of saturation time is also found in quantum circuit complexity, indicating the possible connection between the two complexities [64, 65]. In the monitored case, the quantum complexity profile remains invariant under measurement rate p . In Floquet unitary classes, we probe thermal and local phases using late time saturation of complexity. More specifically, inhomogeneous Gaussian circuits exhibit Anderson localization while strongly coupled spins show many-body localization. The operator complexity can equally be studied and be used to probe thermal and local phases. Similar to the

state complexity, the operator complexity is expected to undergo linear to sublinear transition, before it saturates at exponentially large times $t_{\text{sat}} \sim 4^N$ to a value which grows exponentially with system size $\sim 4^N/2$.

In summary, we discuss in this letter

- How Krylov spread complexity can be defined for discrete time-dependent random circuits. In doing so, one needs to compute the overlap between the state after a certain layer with the corresponding basis vectors and then treat these overlaps as the wavefunctions in the Krylov basis.
- How the complexity profile, saturation values, and the saturation times scale with system size, indicating a connection with the circuit complexity.
- How the complexity profile changes under randomized measurements. We find that with increasing rate of measurement, after a certain system size dependent threshold of measurement rate p_{thr} , the complexity saturation time goes through a sharp increase. For a larger system size N , beyond p_{thr} , the ratio t_{sat}/t_0 is more.
- In floquet setups, how this notion of complexity in the Krylov basis, generated by the unitaries in the discrete-time picture acts as a novel probe of various kinds of localization (Anderson and MBL) through suppression of the saturation value. This notion of complexity therefore still measures the delocalization of the wave function in the state Hilbert space.

There are a number of questions that remain to be answered in future works. A pressing one is if its possible to probe scrambling transition in the monitored RUCs more precisely using quantum complexity. The definition of complexity allows it to grow even in the absence of any growth in entanglement. For example, a discrete evolution in which a product state evolves to another product state results in the growth of complexity but not entanglement. A possible way could be to consider radiative random unitary circuits [44], which were previously shown to exhibit scrambling transition probed using OTOCs.

Acknowledgement.— We would like to thank Vijay Balasubramanian, Sumilan Banerjee, Mario Flory, Shane Kelly, Subroto Mukherjee, and Zahra Raissi for useful discussions. The work of A.B. is supported by the Polish National Science Centre (NCN) grant 2021/42/E/ST2/00234. This research was supported in part by the International Centre for Theoretical Sciences (ICTS) for participating in the program - Quantum Information, Quantum Field Theory and Gravity" (code: ICTS/qftg2024/08). Research at Perimeter Institute is

supported in part by the Government of Canada through the Department of Innovation, Science and Economic Development and by the Province of Ontario through the Ministry of Colleges and Universities.

Bound on saturation time. — To bound the saturation time in case of monitored unitary quantum circuits, we consider the limiting case in which the probability rate is exactly one *i.e.* each qubit is measured after state evolution step. Since during each evolution step, the state evolves through Haar-random unitary and then undergoes measurement, this situation is equivalent to drawing n basis from the basis set $|\{i\}\rangle$ with probability $p(|\{i\}\rangle) = 1/D$. Here $|\{i\}\rangle$ with $i = 0, 1, \dots, D-1$ represents computational basis. The saturation time corresponds to when the Krylov basis form a complete basis vector over complete Hilbert space. In other words, the number of draws required t_s such that each basis vector $|\{i\}\rangle$ is drawn at least once. The probability of drawing D basis vector at least once in n number of drawn can be written as

$$P(n, D) = \frac{D!}{D^n} \mathcal{S}(n, D) \quad (17)$$

where $\mathcal{S}(n, m)$ represents the Stirling partition number which tells the number of ways to partition a set of n objects into m non-empty subsets. We can set the probability $P(n, D) \approx 1 - \epsilon$ for $n \sim D \log(D/\epsilon)$ where $\epsilon \in \{0, 1\}$ represents approximation error. Therefore, the saturation time $t_s < \mathcal{O}(D \log(D/\epsilon))$.

The minimal complexity growth can also be deduced from this limiting case. We consider the probability of drawing m basis vector at least once in n number of drawn given by

$$P(n, m) = \binom{D}{m} \frac{\mathcal{S}(n, m) \cdot m!}{d^n}. \quad (18)$$

Therefore, the complexity can be written as

$$\min \mathbb{E}(\mathcal{C}(t)) = \sum_{i=0}^t iP(t) \quad (19)$$

$$\cong m_{\max} P(t, m_{\max})$$

where m_{\max} corresponds to value of m for which $P(n, m)$ is maximum. To find m_{\max} , we examine the ratio $P(n, m+1)/P(n, m)$

$$\frac{P(n, m+1)}{P(n, m)} = \frac{D-m}{m+1} \cdot \frac{\mathcal{S}(n, m+1)}{\mathcal{S}(n, m)} \quad (20)$$

The maximum occurs when ratio transitions from > 1 to < 1 , *i.e.*, $P(n, m+1) \approx P(n, m)$. If we consider n to be large, we can further approximate

$$\mathcal{S}(n, m) \underset{n \rightarrow \infty}{\sim} m^n / m!$$

so that

$$\frac{P(n, m+1)}{P(n, m)} \sim \frac{D-m}{(m+1)^2} \left(1 + \frac{1}{m}\right)^n \quad (21)$$

$$\sim \frac{Dn}{m^3}$$

where, in the last step, we assumed $D \gg m \gg 1$. Therefore, $m_{\max} \sim n^{1/3}$ leading to sub-linear complexity grow $\sim t^{1/3}$.

[†] hsahu@pitp.ca

[§] aranya.bhattacharya@uj.edu.pl

[‡] pingalnath@iisc.ac.in

- [1] P. Nandy, A. S. Matsoukas-Roubeas, P. Martínez-Azcona, A. Dymarsky, and A. del Campo, *Quantum Dynamics in Krylov Space: Methods and Applications* (2024), arXiv:2405.09628 [quant-ph].
- [2] B. Swingle, *Nature Physics* **14**, 988 (2018).
- [3] S. Sahu, S. Xu, and B. Swingle, *Phys. Rev. Lett.* **123**, 165902 (2019).
- [4] D. Harlow and P. Hayden, *Journal of High Energy Physics* **2013**, 85 (2013).
- [5] Patrick Hayden and John Preskill, *Journal of High Energy Physics* **2007**, 120 (2007).
- [6] S. H. Shenker and D. Stanford, *Journal of High Energy Physics* **2015**, 132 (2015).
- [7] S. H. Shenker and D. Stanford, *Journal of High Energy Physics* **2014**, 67 (2014).
- [8] Yasuhiro Sekino and L. Susskind, *Journal of High Energy Physics* **2008**, 065 (2008).
- [9] J. Maldacena, S. H. Shenker, and D. Stanford, *Journal of High Energy Physics* **2016**, 106 (2016).
- [10] P. Hosur, X.-L. Qi, D. A. Roberts, and B. Yoshida, *Journal of High Energy Physics* **2016**, 4 (2016).
- [11] D. A. Roberts and B. Yoshida, *Journal of High Energy Physics* **2017**, 121 (2017).
- [12] J. R. McClean, S. Boixo, V. N. Smelyanskiy, R. Babush, and H. Neven, *Nature Communications* **9**, 4812 (2018).
- [13] J. Haferkamp, F. Montealegre-Mora, M. Heinrich, J. Eisert, D. Gross, and I. Roth, *Communications in Mathematical Physics* **397**, 995 (2023).
- [14] E. Knill, D. Leibfried, R. Reichle, J. Britton, R. B. Blakestad, J. D. Jost, C. Langer, R. Ozeri, S. Seidelin, and D. J. Wineland, *Phys. Rev. A* **77**, 012307 (2008).
- [15] C. Murthy and M. Srednicki, *Phys. Rev. Lett.* **123**, 230606 (2019).
- [16] M. Srednicki, *Phys. Rev. E* **50**, 888 (1994).
- [17] S. Xu and B. Swingle, *PRX Quantum* **5**, 010201 (2024).
- [18] R. J. Lewis-Swan, A. Safavi-Naini, A. M. Kaufman, and A. M. Rey, *Nature Reviews Physics* **1**, 627 (2019).
- [19] J. Maldacena and D. Stanford, *Phys. Rev. D* **94**, 106002 (2016).
- [20] J. Polchinski and V. Rosenhaus, *Journal of High Energy Physics* **2016**, 1 (2016).
- [21] R. Belyansky, P. Bienias, Y. A. Kharkov, A. V. Gorshkov, and B. Swingle, *Phys. Rev. Lett.* **125**, 130601 (2020).
- [22] L. Susskind, *Fortschritte der Physik* **64**, 24 (2016).

- [23] D. Stanford and L. Susskind, *Phys. Rev. D* **90**, 126007 (2014).
- [24] A. R. Brown, D. A. Roberts, L. Susskind, B. Swingle, and Y. Zhao, *Phys. Rev. D* **93**, 086006 (2016).
- [25] A. R. Brown and L. Susskind, *Phys. Rev. D* **97**, 086015 (2018).
- [26] A. R. Brown, D. A. Roberts, L. Susskind, B. Swingle, and Y. Zhao, *Phys. Rev. Lett.* **116**, 191301 (2016).
- [27] J. Haferkamp, P. Faist, N. B. T. Kothakonda, J. Eisert, and N. Yunger Halpern, *Nature Physics* **18**, 528 (2022).
- [28] D. E. Parker, X. Cao, A. Avdoshkin, T. Scaffidi, and E. Altman, *Phys. Rev. X* **9**, 041017 (2019).
- [29] V. Balasubramanian, P. Caputa, J. M. Magan, and Q. Wu, *Phys. Rev. D* **106**, 046007 (2022).
- [30] P. Caputa and S. Liu, *Phys. Rev. B* **106**, 195125 (2022).
- [31] E. Rabinovici, A. Sánchez-Garrido, R. Shir, and J. Sonner, *JHEP* **06**, 062, arXiv:2009.01862 [hep-th].
- [32] P. Caputa and S. Datta, *JHEP* **12**, 188, [Erratum: *JHEP* **09**, 113 (2022)], arXiv:2110.10519 [hep-th].
- [33] F. B. Trigueros and C.-J. Lin, *SciPost Phys.* **13**, 037 (2022), arXiv:2112.04722 [cond-mat.dis-nn].
- [34] A. Bhattacharya, P. Nandy, P. P. Nath, and H. Sahu, *JHEP* **12**, 081, arXiv:2207.05347 [quant-ph].
- [35] A. Bhattacharya, P. Nandy, P. P. Nath, and H. Sahu, *JHEP* **12**, 066, arXiv:2303.04175 [quant-ph].
- [36] P. Caputa, N. Gupta, S. S. Haque, S. Liu, J. Murugan, and H. J. R. Van Zyl, *Journal of High Energy Physics* **2023**, 120 (2023).
- [37] E. Rabinovici, A. Sánchez-Garrido, R. Shir, and J. Sonner, *JHEP* **03**, 211, arXiv:2112.12128 [hep-th].
- [38] A. Bhattacharya, P. P. Nath, and H. Sahu, *Phys. Rev. D* **109**, 066010 (2024).
- [39] A. Bhattacharya and A. Jana, Quantum chaos and complexity from string scattering amplitudes (2024), arXiv:2408.11096 [hep-th].
- [40] J. L. F. Barbón, E. Rabinovici, R. Shir, and R. Sinha, *JHEP* **10**, 264, arXiv:1907.05393 [hep-th].
- [41] M. Ganguli and A. Jana, State Dependent Spread Complexity Dynamics in Many-Body Localization Transition (2024), arXiv:2409.02186 [cond-mat.dis-nn].
- [42] K. Takahashi and A. del Campo, *Phys. Rev. Lett.* **134**, 030401 (2025).
- [43] B. Skinner, J. Ruhman, and A. Nahum, *Phys. Rev. X* **9**, 031009 (2019).
- [44] Z. Weinstein, S. P. Kelly, J. Marino, and E. Altman, *Phys. Rev. Lett.* **131**, 220404 (2023).
- [45] Y. Bao, S. Choi, and E. Altman, *Phys. Rev. B* **101**, 104301 (2020).
- [46] Y. Li, X. Chen, and M. P. A. Fisher, *Phys. Rev. B* **100**, 134306 (2019).
- [47] S. Choi, Y. Bao, X.-L. Qi, and E. Altman, *Phys. Rev. Lett.* **125**, 030505 (2020).
- [48] M. J. Gullans and D. A. Huse, *Phys. Rev. X* **10**, 041020 (2020).
- [49] M. J. Gullans and D. A. Huse, *Phys. Rev. Lett.* **125**, 070606 (2020).
- [50] Y. Li, Y. Zou, P. Glorioso, E. Altman, and M. P. A. Fisher, *Phys. Rev. Lett.* **130**, 220404 (2023).
- [51] A. Nahum, J. Ruhman, S. Vijay, and J. Haah, *Phys. Rev. X* **7**, 031016 (2017).
- [52] A. Nahum, S. Vijay, and J. Haah, *Phys. Rev. X* **8**, 021014 (2018).
- [53] C. W. von Keyserlingk, T. Rakovszky, F. Pollmann, and S. L. Sondhi, *Phys. Rev. X* **8**, 021013 (2018).
- [54] T. Rakovszky, F. Pollmann, and C. W. von Keyserlingk, *Phys. Rev. X* **8**, 031058 (2018).
- [55] V. Khemani, A. Vishwanath, and D. A. Huse, *Phys. Rev. X* **8**, 031057 (2018).
- [56] A. Chan, A. De Luca, and J. T. Chalker, *Phys. Rev. X* **8**, 041019 (2018).
- [57] C. Sünderhauf, D. Pérez-García, D. A. Huse, N. Schuch, and J. I. Cirac, *Phys. Rev. B* **98**, 134204 (2018).
- [58] N. Lashkari, D. Stanford, M. Hastings, T. Osborne, and P. Hayden, *Journal of High Energy Physics* **2013**, 22 (2013).
- [59] R. Jozsa and A. Miyake, *Proceedings of the Royal Society A: Mathematical, Physical and Engineering Sciences* **464**, 3089 (2008), publisher: Royal Society.
- [60] S. Bravyi, *Quantum Info. Comput.* **5**, 216–238 (2005).
- [61] H. Sahu, *Phys. Rev. A* **110**, 052405 (2024).
- [62] R. Suzuki, J. Haferkamp, J. Eisert, and P. Faist, *Quantum* **9**, 1627 (2025).
- [63] R. Nandkishore and D. A. Huse, *Annual Review of Condensed Matter Physics* **6**, 15 (2015).
- [64] B. Craps, O. Evnin, and G. Pascuzzi, *Phys. Rev. Lett.* **132**, 160402 (2024).
- [65] A. Bhattacharya, H. Sahu, A. Zahed, and K. Sen, *Phys. Rev. A* **109**, 022223 (2024).